

## A WEAKLY OVER-PENALIZED SYMMETRIC INTERIOR PENALTY METHOD\*

SUSANNE C. BRENNER<sup>†</sup>, LUKE OWENS<sup>‡</sup>, AND LI-YENG SUNG<sup>§</sup>

**Abstract.** We introduce a new symmetric interior penalty method for symmetric positive definite second order elliptic boundary value problems, where the jumps across element boundaries are weakly over-penalized. Error estimates are derived in the energy norm and the  $L_2$  norm for both conforming and nonconforming meshes. Numerical results illustrating the performance of the method are also presented.

**Key words.** symmetric interior penalty method, weak over-penalization

**AMS subject classifications.** 65N30

**1. Introduction.** In this paper we study a new symmetric interior penalty method for second order symmetric positive-definite elliptic boundary value problems. For simplicity, we focus on a two dimensional model problem, but the results can be extended to more general problems and three dimensional domains.

Let  $\Omega \subset \mathbb{R}^2$  be a bounded polygonal domain. Consider the weak formulation of the Poisson problem with Dirichlet boundary condition:

Find  $u \in H^1(\Omega)$  such that

$$(1.1a) \quad a(u, v) = \int_{\Omega} f v \, dx \quad \forall v \in H_0^1(\Omega),$$

$$(1.1b) \quad u = \varphi \quad \text{on } \partial\Omega,$$

where  $f \in L_2(\Omega)$ ,  $\varphi \in H^2(\Omega)$  and

$$(1.2) \quad a(w, v) = \int_{\Omega} \nabla w \cdot \nabla v \, dx.$$

This problem can be solved numerically by symmetric or nonsymmetric interior penalty methods. Let  $\mathcal{T}_h$  be a simplicial triangulation of  $\Omega$  with mesh parameter

$$h = \max_{T \in \mathcal{T}_h} \text{diam } T,$$

and  $V_h$  be the discontinuous  $P_1$  finite element space associated with  $\mathcal{T}_h$ , i.e.,

$$V_h = \{v \in L_2(\Omega) : v|_T = v|_T \in P_1(T) \quad \forall T \in \mathcal{T}_h\}.$$

---

\*Received October 3, 2007. Accepted for publication February 20, 2008. Published online on May 29, 2008. Recommended by Y. Achdou.

<sup>†</sup>Department of Mathematics and Center for Computation and Technology, Louisiana State University, Baton Rouge, LA 70803 ([brenner@math.lsu.edu](mailto:brenner@math.lsu.edu)). The work of this author was supported in part by the National Science Foundation under Grant No. DMS-03-11790 and the Humboldt Foundation through her Humboldt Research Award.

<sup>‡</sup>Department of Mathematics, University of South Carolina, Columbia, SC 29208 ([owens1@math.sc.edu](mailto:owens1@math.sc.edu)). The work of this author was supported in part by the National Science Foundation under Grant No. DMS-03-11790.

<sup>§</sup>Department of Mathematics, Louisiana State University, Baton Rouge, LA 70803 ([sung@math.lsu.edu](mailto:sung@math.lsu.edu)).

The discrete problems for the standard interior penalty methods are:

Find  $u_h^\pm$  such that

$$a_h^\pm(u_h^\pm, v) = \int_{\Omega} f v \, dx \pm \sum_{e \in \mathcal{E}_h^b} \int_e \{\{\nabla v\}\} \cdot [[\varphi]] \, ds + \sum_{e \in \mathcal{E}_h^b} \frac{\eta}{|e|} \int_e [[\varphi]] \cdot [[v]] \, ds \quad \forall v \in V_h,$$

where the bilinear form  $a_h^\pm(\cdot, \cdot)$  is defined by

$$\begin{aligned} a_h^\pm(w, v) = & \sum_{T \in \mathcal{T}_h} \int_T \nabla w \cdot \nabla v \, dx - \sum_{e \in \mathcal{E}_h} \int_e \{\{\nabla w\}\} \cdot [[v]] \, ds \\ & \pm \sum_{e \in \mathcal{E}_h} \int_e \{\{\nabla v\}\} \cdot [[w]] \, ds + \sum_{e \in \mathcal{E}_h} \frac{\eta}{|e|} \int_e [[w]] \cdot [[v]] \, ds. \end{aligned}$$

Here  $\mathcal{E}_h$  (resp.  $\mathcal{E}_h^b$ ) is the set of the edges (resp. boundary edges) in  $\mathcal{T}_h$ ,  $|e|$  is the length of  $e$ ,  $\{\{\nabla v\}\}$  denotes the mean of the gradient of  $v$  (which is defined to be the gradient of  $v$  on a boundary edge),  $[[v]]$  denotes the jump of  $v$ , and  $\eta > 0$  is a penalty parameter.

Note that the jump of a function is actually a vector [4]. More precisely, let  $e$  be an interior edge shared by the triangles  $T_{e,1}, T_{e,2} \in \mathcal{T}_h$ . Then we define on  $e$ ,

$$[[v]] = v_1 \mathbf{n}_{e,1} + v_2 \mathbf{n}_{e,2},$$

where  $v_1 = v|_{T_{e,1}}$ ,  $v_2 = v|_{T_{e,2}}$  and  $\mathbf{n}_{e,1}$  (resp.  $\mathbf{n}_{e,2}$ ) is the unit normal of  $e$  pointing towards the outside of  $T_{e,1}$  (resp.  $T_{e,2}$ ). On an edge  $e$  along  $\partial\Omega$ , we define

$$[[v]] = (v|_e) \mathbf{n}_e,$$

where  $\mathbf{n}_e$  is the unit normal of  $e$  pointing outside  $\Omega$ .

The discrete function  $u_h^-$  is the solution of the symmetric interior penalty method [27, 3] and  $u_h^+$  is the solution of the nonsymmetric interior penalty method [26]. Both methods are consistent in the sense that

$$a_h^\pm(u, v) = \int_{\Omega} f v \, dx \pm \sum_{e \in \mathcal{E}_h^b} \int_e \{\{\nabla v\}\} \cdot [[\varphi]] \, ds + \sum_{e \in \mathcal{E}_h^b} \frac{\eta}{|e|} \int_e [[\varphi]] [[v]] \, ds \quad \forall v \in V_h.$$

The nonsymmetric method is stable for any positive  $\eta$ , and the symmetric method is stable if  $\eta$  is sufficiently large. Therefore  $u_h^\pm$  (when the methods are stable) satisfy a quasi-optimal error estimate in the norm  $\|\cdot\|_h$  defined by

$$(1.3) \quad \|v\|_h^2 = \sum_{T \in \mathcal{T}_h} \|\nabla v\|_{L_2(T)}^2 + \sum_{e \in \mathcal{E}_h} |e| \|\{\{\nabla v\}\}\|_{L_2(e)}^2 + \eta \sum_{e \in \mathcal{E}_h} |e|^{-1} \|[[v]]\|_{L_2(e)}^2.$$

In particular, we have

$$\|u - u_h^\pm\|_h \leq C \inf_{v \in V_h} \|u - v\|_h,$$

where  $C > 0$  depends only on the shape regularity of  $\mathcal{T}_h$ , as long as the penalty parameter satisfies the condition

$$(1.4) \quad \eta \geq \eta_0 > 0.$$

For the symmetric method the lower bound  $\eta_0$  for the penalty parameter must be sufficiently large, while for the nonsymmetric method it can be arbitrary. From here on we use  $C$  to denote a generic positive constant that can take different values at different occurrences.

The fact that the stability of the symmetric method requires the tuning of a penalty parameter can be considered a drawback of the method. On the other hand, the symmetric method is adjoint consistent while the nonsymmetric method is not. Hence the  $L_2$  error for  $u_h^-$  gains a power of  $h$  (depending on the elliptic regularity) over the error in  $\|\cdot\|_h$ , but there is no such gain for the  $L_2$  error of  $u_h^+$ .

Our goal is to develop a symmetric interior penalty method that satisfies the correct error estimates in both the energy norm and the  $L_2$  norm, and at the same time is stable for any choice of the penalty parameter. This is achieved by abandoning the consistency of the method and at the same time applying a weak over-penalization to the jumps of the discontinuous finite element functions across the edges. The discrete problem of the weakly over-penalized symmetric interior penalty (WOPSIP) method is: Find  $u_h \in V_h$  such that

$$(1.5) \quad a_h(u_h, v) = \int_{\Omega} f v \, dx + \eta \sum_{e \in \mathcal{E}_h^b} \frac{1}{|e|^3} \int_e \Pi_e^0[[\varphi]] \cdot \Pi_e^0[[v]] \, ds \quad \forall v \in V_h,$$

where

$$(1.6) \quad a_h(w, v) = \sum_{T \in \mathcal{T}_h} \int_T \nabla w \cdot \nabla v \, dx + \eta \sum_{e \in \mathcal{E}_h} \frac{1}{|e|^3} \int_e \Pi_e^0[[w]] \cdot \Pi_e^0[[v]] \, ds,$$

$\Pi_e^0$  is the orthogonal projection from  $[L_2(e)]^2$  onto  $[P_0(e)]^2$  (the space of constant vectors on  $e$ ), and the penalty parameter  $\eta$  satisfies (1.4) for an arbitrary positive lower bound  $\eta_0$ .

Intuitively, the weak over-penalization forces the scheme (1.5) to behave like the classical nonconforming  $P_1$  finite element method [20], which is known to satisfy the correct error estimates for the Poisson problem. Of course, unlike the classical nonconforming  $P_1$  finite element method, the WOPSIP method can handle meshes with hanging nodes. It is important to note that the ill-conditioning resulting from the over-penalization can be remedied by a simple block-diagonal preconditioner (see Section 5 below).

**REMARK 1.1.** A symmetric interior penalty method was introduced in [7], where an appropriate lifting of the jump was penalized. It is equivalent to the approach in [27, 3] with a built-in edge-by-edge numerical estimate of the penalty parameter. Consequently, the lower bound for the penalty parameter in the approach of [7] becomes explicit (cf. the discussion in [4]). In contrast, the stability of the WOPSIP method does not require an edge-by-edge numerical estimate of the penalty parameter.

The rest of the paper is organized as follows. We first review the regularity of the solution of (1.1) in Section 2. We then establish energy error estimates in Section 3 and  $L_2$  error estimates in Section 4. In Section 5 we construct a simple block-diagonal preconditioner that offsets the ill-conditioning due to the weak over-penalization in (1.6). The extension of these results to grids with hanging nodes and equations with variable coefficients is given in Section 6. Numerical results are reported in Section 7, followed by some concluding remarks in Section 8.

**2. Regularity.** The analysis of the scheme (1.5) involves the regularity of the solution  $u$  of (1.1), which we briefly summarize below. Details can be found in [23, 21, 24].

Let  $c_1, \dots, c_L$  be the corners of  $\Omega$  and  $\omega_\ell$  be the (interior) angle at  $c_\ell$ . We can write

$$(2.1) \quad u = u_R + u_S,$$

where the regular part  $u_R \in H^2(\Omega)$  and the singular part  $u_S$  is supported near the reentrant corners of  $\Omega$ . More precisely, let  $\delta > 0$  be small enough so that the neighborhoods

$$\mathcal{N}_{\ell,\delta} = \{x \in \Omega : |x - c_\ell| < \delta\} \quad \text{for } 1 \leq \ell \leq L$$

are disjoint. Then we have

$$(2.2) \quad u_S = \sum_{\omega_\ell > \pi} \kappa_\ell r_\ell^{\pi/\omega_\ell} \sin((\pi/\omega_\ell)\theta) \chi(r_\ell),$$

where  $(r_\ell, \theta_\ell)$  are the local polar coordinates at  $c_\ell$  such that the two edges emanating from  $c_\ell$  are given by  $\theta_\ell = 0$  and  $\theta_\ell = \omega_\ell$ ,  $\kappa_\ell \in \mathbb{R}$  is the (generalized) stress intensity factor at  $c_\ell$ , and  $\chi(t)$  is a smooth cut-off function that equals 1 for  $t \leq \delta/2$  and vanishes for  $t > 3\delta/4$ .

It follows from the singular function representation (2.1) and the definition (2.2) of the singular part that

$$u \in H^2(\Omega) \quad \text{if } \Omega \text{ is convex} \quad \text{and} \quad u \in H^{1+(\pi/\omega)-\epsilon}(\Omega) \quad \text{if } \Omega \text{ is nonconvex,}$$

where  $\omega$  is the maximum of the interior angles at the reentrant corners and  $\epsilon$  is any positive number. More precisely, when  $\Omega$  is nonconvex,  $u$  is  $H^2$  away from the reentrant corners of  $\Omega$ , and at the reentrant corner  $c_\ell$ ,

$$u \in H^{1+(\pi/\omega_\ell)-\epsilon}(\mathcal{N}_{\ell,\delta}) \quad \text{for any } \epsilon > 0.$$

Furthermore, we have

$$(2.3) \quad \|u\|_{H^2(\Omega)} \leq C(\|f\|_{L_2(\Omega)} + \|\varphi\|_{H^2(\Omega)})$$

if  $\Omega$  is convex. For a nonconvex  $\Omega$ , we have

$$(2.4) \quad \|u\|_{H^{1+\alpha}(\Omega)} \leq C_\alpha(\|f\|_{L_2(\Omega)} + \|\varphi\|_{H^2(\Omega)}),$$

where  $\alpha$  is any number strictly less than  $1 + (\pi/\omega)$ ,

$$(2.5) \quad \|u_R\|_{H^2(\Omega)} + \sum_{\omega_\ell > \pi} |\kappa_\ell| \leq C(\|f\|_{L_2(\Omega)} + \|\varphi\|_{H^2(\Omega)}),$$

and, at a reentrant corner  $c_\ell$ ,

$$(2.6) \quad \|u\|_{H^{1+(\pi/\omega_\ell)-\epsilon}(\mathcal{N}_{\ell,\delta})} \leq C_\epsilon(\|f\|_{L_2(\Omega)} + \|\varphi\|_{H^2(\Omega)}).$$

A useful consequence of the representation (2.1) is the following lemma on integration by parts involving  $u$ .

LEMMA 2.1. *Let  $u$  be the solution of (1.1),  $T \in \mathcal{T}_h$  and  $v \in H^1(T)$ . Then we have*

$$(2.7) \quad \int_T \nabla u \cdot \nabla v \, dx = \int_{\partial T} \nabla u \cdot v \mathbf{n} \, ds + \int_T f v \, dx,$$

where  $\mathbf{n}$  is the unit outward normal along  $\partial T$ .

*Proof.* Since  $C^1(\bar{T})$  is dense in  $H^1(\Omega)$  and all three terms in (2.7) are bounded linear functionals on  $H^1(\Omega)$  (because  $u \in H^{1+\alpha}(\Omega)$  for some  $\alpha > 1/2$ ), it suffices to prove (2.7) for  $v \in C^1(\bar{T})$ .

If  $T$  does not touch any of the reentrant corners of  $\Omega$ , then  $u \in H^2(T)$ ,  $-\Delta u = f$  in  $T$  and (2.7) is standard.

Suppose only one of the vertex of  $T$  is a reentrant corner  $c_\ell$  of  $\Omega$ . (The case where more than one of the vertices of  $T$  are reentrant corners can be handled similarly.) For a sufficiently small positive number  $\gamma$ , we have the standard integration by parts formula

$$(2.8) \quad \int_{T_\gamma} \nabla u \cdot \nabla v \, dx = \int_{\partial T_\gamma} \nabla u \cdot v \mathbf{n} \, ds + \int_{T_\gamma} f v \, dx,$$

where  $T_\gamma = \{x \in T : |x - c_\ell| > \gamma\}$ . We can recover (2.7) by letting  $\gamma \downarrow 0$  in (2.8), provided that we have

$$(2.9) \quad \lim_{\gamma \downarrow 0} \int_{A_\gamma} \nabla u \cdot v \mathbf{n} \, ds = 0,$$

where  $A_\gamma$  is the arc  $\{x \in T : |x - c_\ell| = \gamma\}$ .

In order to prove (2.9), we use (2.1) and (2.2) to write

$$\nabla u \cdot \mathbf{n} = \nabla u_R \cdot \mathbf{n} - \kappa_\ell (\pi/\omega_\ell) r^{(\pi/\omega_\ell)-1} \sin((\omega_\ell/\pi)\theta),$$

and hence, by the Cauchy-Schwarz inequality, the trace theorem and direct calculation,

$$\begin{aligned} \left| \int_{A_\gamma} \nabla u \cdot v \mathbf{n} \, ds \right| &\leq (\|\nabla u_R \cdot \mathbf{n}\|_{L^1(A_\gamma)} + |\kappa_\ell| (\pi/\omega_\ell) \gamma^{\pi/\omega_\ell} \omega_\ell) \|v\|_{L^\infty(T)} \\ &\leq ((\gamma \omega_\ell)^{1/2} \|\nabla u_R \cdot \mathbf{n}\|_{L^2(A_\gamma)} + |\kappa_\ell| (\pi/\omega_\ell) \gamma^{\pi/\omega_\ell} \omega_\ell) \|v\|_{L^\infty(T)} \\ &\leq (C(\gamma \omega_\ell)^{1/2} \|u_R\|_{H^2(T)} + |\kappa_\ell| (\pi/\omega_\ell) \gamma^{\pi/\omega_\ell} \omega_\ell) \|v\|_{L^\infty(T)}, \end{aligned}$$

which immediately implies (2.9).  $\square$

The following trace estimates are consequences of the trace theorem and scaling:

$$(2.10) \quad |e|^{-1} \|v\|_{L^2(\partial T)}^2 \leq C (h_T^{-2} \|v\|_{L^2(T)}^2 + \|\nabla v\|_{L^2(T)}^2),$$

$$(2.11) \quad |e| \|\nabla v\|_{L^2(\partial T)}^2 \leq C_s (\|\nabla v\|_{L^2(T)}^2 + h_T^{2s} |\nabla v|_{H^s(T)}^2),$$

where  $s$  is any number in the interval  $(1/2, 1]$ . In view of (2.3), (2.4) and (2.11), we have

$$(2.12) \quad \sum_{e \in \mathcal{E}_h} |e| \|\nabla u\|_{L^2(e)}^2 \leq C (\|f\|_{L^2(\Omega)}^2 + \|\varphi\|_{H^2(\Omega)}^2).$$

**3. Energy error estimates.** Let the mesh-dependent norm  $\|\cdot\|_h$  be defined by

$$(3.1) \quad \|v\|_h^2 = \sum_{T \in \mathcal{T}_h} \|\nabla v\|_{L^2(T)}^2 + \sum_{e \in \mathcal{E}_h} |e| \|\{\!\{ \nabla v \}\!\}\|_{L^2(e)}^2 + \eta \sum_{e \in \mathcal{E}_h} |e|^{-3} \|\Pi_e^0[v]\|_{L^2(e)}^2.$$

For  $v \in V_h$ , since  $\{\!\{ \nabla v \}\!\}$  is a constant vector on each  $e$ , it is easy to see that

$$\sum_{e \in \mathcal{E}_h} |e| \|\{\!\{ \nabla v \}\!\}\|_{L^2(e)}^2 \leq C \sum_{T \in \mathcal{T}_h} \|\nabla v\|_{L^2(T)}^2 \quad \forall v \in V_h,$$

and hence, in view of (1.6),

$$(3.2) \quad C \|v\|_h^2 \leq a_h(v, v) \quad \forall v \in V_h.$$

In the other direction, we have the obvious estimate

$$(3.3) \quad a_h(w, v) \leq \|w\|_h \|v\|_h$$

for all  $v, w$  that are piecewise  $H^s$  with respect to  $\mathcal{T}_h$  for some  $s > 3/2$ .

Furthermore, the norm  $\|\cdot\|_h$  dominates the norm  $\|\cdot\|_h$  defined in (1.3) because of the following lemma.

LEMMA 3.1. *There exists a positive constant  $C$ , depending only on the shape regularity of  $\mathcal{T}_h$  and  $\eta_0$ , such that*

$$(3.4) \quad \sum_{e \in \mathcal{E}_h} |e|^{-1} \|\llbracket v \rrbracket\|_{L_2(e)}^2 \leq C \left\{ \sum_{T \in \mathcal{T}_h} \|\nabla v\|_{L_2(T)}^2 + \sum_{e \in \mathcal{E}_h} |e|^{-1} \|\Pi_e^0 \llbracket v \rrbracket\|_{L_2(e)}^2 \right\} \leq C \|v\|_h^2$$

for any  $v$  that is piecewise  $H^1$  with respect to  $\mathcal{T}_h$ .

*Proof.* Let  $\bar{v}$  be the piecewise constant function that takes the mean value of  $v$  on each  $T \in \mathcal{T}_h$ . We have, by (2.10) and a standard interpolation error estimate [19, 18],

$$\begin{aligned} \sum_{e \in \mathcal{E}_h} |e|^{-1} \|\llbracket v \rrbracket\|_{L_2(e)}^2 &\leq 2 \sum_{e \in \mathcal{E}_h} |e|^{-1} \left( \|\llbracket v - \bar{v} \rrbracket\|_{L_2(e)}^2 + \|\llbracket \bar{v} \rrbracket\|_{L_2(e)}^2 \right) \\ &\leq C \sum_{T \in \mathcal{T}_h} \|\nabla v\|_{L_2(T)}^2 + 2 \sum_{e \in \mathcal{E}_h} |e|^{-1} \|\Pi_e^0 \llbracket \bar{v} \rrbracket\|_{L_2(e)}^2 \\ &\leq C \sum_{T \in \mathcal{T}_h} \|\nabla v\|_{L_2(T)}^2 + 4 \sum_{e \in \mathcal{E}_h} |e|^{-1} \left( \|\Pi_e^0 \llbracket \bar{v} - v \rrbracket\|_{L_2(e)}^2 + \|\Pi_e^0 \llbracket v \rrbracket\|_{L_2(e)}^2 \right) \\ &\leq C \sum_{T \in \mathcal{T}_h} \|\nabla v\|_{L_2(T)}^2 + 4 \sum_{e \in \mathcal{E}_h} |e|^{-1} \|\Pi_e^0 \llbracket v \rrbracket\|_{L_2(e)}^2. \quad \square \end{aligned}$$

The following lemma provides an abstract estimate for the discretization error in the mesh-dependent norm  $\|\cdot\|_h$ .

LEMMA 3.2. *Let  $u \in H^1(\Omega)$  (resp.  $u_h \in V_h$ ) be the solution of (1.1) (resp. (1.5)). Then the following error estimate holds:*

$$(3.5) \quad \|u - u_h\|_h \leq C \left[ \inf_{v \in V_h} \|u - v\|_h + h(\|f\|_{L_2(\Omega)} + \|\varphi\|_{H^2(\Omega)}) \right].$$

*Proof.* Let  $v \in V_h$  be arbitrary. It follows from (3.2) and (3.3) that

$$(3.6) \quad \begin{aligned} \|u - u_h\|_h &\leq \|u - v\|_h + \|v - u_h\|_h \\ &\leq \|u - v\|_h + C \max_{w \in V_h \setminus \{0\}} \frac{a_h(v - u_h, w)}{\|w\|_h} \\ &\leq C \left\{ \|u - v\|_h + \max_{w \in V_h \setminus \{0\}} \frac{a_h(u - u_h, w)}{\|w\|_h} \right\}. \end{aligned}$$

From (1.1a), (1.2), (1.5), (1.6) and Lemma 2.1, we have

$$(3.7) \quad \begin{aligned} a_h(u - u_h, w) &= \sum_{e \in \mathcal{E}_h} \int_e \nabla u \cdot \llbracket w \rrbracket ds \\ &= \sum_{e \in \mathcal{E}_h} \int_e \{\{\nabla(u - v)\}\} \cdot \llbracket w \rrbracket ds + \sum_{e \in \mathcal{E}_h} \int_e \{\{\nabla v\}\} \cdot \Pi_e^0 \llbracket w \rrbracket ds. \end{aligned}$$

Using (2.12), (3.1), (3.4) and the Cauchy-Schwarz inequality, the two terms on the right-hand side of (3.7) can be estimated as follows:

$$\sum_{e \in \mathcal{E}_h} \int_e \{\{\nabla(u - v)\}\} \cdot \llbracket w \rrbracket ds$$

$$\begin{aligned}
(3.8) \quad & \leq \left( \sum_{e \in \mathcal{E}_h} |e| \|\{\!\!\{ \nabla(u-v) \}\!\!\}\|_{L_2(e)}^2 \right)^{1/2} \left( \sum_{e \in \mathcal{E}_h} |e|^{-1} \|\llbracket w \rrbracket\|_{L_2(e)}^2 \right)^{1/2} \\
& \leq C \|u-v\|_h \|w\|_h, \\
& \sum_{e \in \mathcal{E}_h} \int_e \{\!\!\{ \nabla v \}\!\!\} \cdot \Pi_e^0 \llbracket w \rrbracket ds \\
& \leq \left( \sum_{e \in \mathcal{E}_h} |e|^3 \|\{\!\!\{ \nabla v \}\!\!\}\|_{L_2(e)}^2 \right)^{1/2} \left( \sum_{e \in \mathcal{E}_h} |e|^{-3} \|\Pi_e^0 \llbracket w \rrbracket\|_{L_2(e)}^2 \right)^{1/2} \\
(3.9) \quad & \leq \left( \sum_{e \in \mathcal{E}_h} |e|^3 \|\{\!\!\{ \nabla(v-u) \}\!\!\}\|_{L_2(e)}^2 \right)^{1/2} \left( \sum_{e \in \mathcal{E}_h} |e|^{-3} \|\Pi_e^0 \llbracket w \rrbracket\|_{L_2(e)}^2 \right)^{1/2} \\
& \quad + \left( \sum_{e \in \mathcal{E}_h} |e|^3 \|\{\!\!\{ \nabla u \}\!\!\}\|_{L_2(e)}^2 \right)^{1/2} \left( \sum_{e \in \mathcal{E}_h} |e|^{-3} \|\Pi_e^0 \llbracket w \rrbracket\|_{L_2(e)}^2 \right)^{1/2} \\
& \leq Ch (\|u-v\|_h + \|f\|_{L_2(\Omega)} + \|\varphi\|_{H^2(\Omega)}) \|w\|_h.
\end{aligned}$$

The estimate (3.5) follows from (3.6)–(3.9).  $\square$

In order to derive concrete error estimates from (3.5), we need a good interpolation operator for the finite element space  $V_h$ . Let the Crouzeix-Raviart interpolation operator  $\Pi_T : H^1(T) \rightarrow P_1(T)$  be defined by

$$\int_{e_i} \Pi_T \zeta ds = \int_{e_i} \zeta ds \quad \text{for } i = 1, 2, 3,$$

where  $e_1, e_2$  and  $e_3$  are the three edges of the triangle  $T$ . This weak interpolation operator satisfies the estimate [20]

$$(3.10) \quad \|\zeta - \Pi_T \zeta\|_{L_2(T)} + h_T \|\nabla(\zeta - \Pi_T \zeta)\|_{L_2(T)} \leq Ch_T^{1+\alpha} |\zeta|_{H^{1+\alpha}(T)} \quad \forall \zeta \in H^{1+\alpha}(T),$$

for any  $\alpha$  between 0 and 1, where  $h_T = \text{diam } T$ .

We can define a global interpolation operator  $\Pi_h : H^1(\Omega) \rightarrow V_h$  by piecing the local interpolation operators together:

$$(3.11) \quad (\Pi_h \zeta)_T = \Pi_T(\zeta|_T) \quad \forall T \in \mathcal{T}_h.$$

Note that

$$(3.12) \quad \Pi_e^0 \llbracket \zeta - \Pi_h \zeta \rrbracket = \mathbf{0} \quad \forall \zeta \in H^1(\Omega), e \in \mathcal{E}_h,$$

$$(3.13) \quad \Pi_e^0 \llbracket \Pi_h \zeta \rrbracket = \mathbf{0} \quad \forall \zeta \in H_0^1(\Omega), e \in \mathcal{E}_h.$$

It follows from (3.5) that

$$(3.14) \quad \|u - u_h\|_h \leq C \left[ \|u - \Pi_h u\|_h + h (\|f\|_{L_2(\Omega)} + \|\varphi\|_{H^2(\Omega)}) \right],$$

and, in view of (3.1) and (3.12),

$$(3.15) \quad \|u - \Pi_h u\|_h = \left( \sum_{T \in \mathcal{T}_h} \|\nabla(u - \Pi_h u)\|_{L_2(T)}^2 + \sum_{e \in \mathcal{E}_h} |e| \|\{\!\!\{ \nabla(u - \Pi_h u) \}\!\!\}\|_{L_2(e)}^2 \right)^{1/2}.$$

Using (2.3), (2.4), (2.11), (3.10) and (3.15), we can obtain immediately the following lemma on interpolation errors for  $\Pi_h$ .

LEMMA 3.3. Let  $\mathcal{T}_h$  be a quasi-uniform mesh on  $\Omega$  with mesh parameter  $h = \max_{T \in \mathcal{T}_h} h_T$ . We have the following interpolation error estimates:

$$(3.16) \quad \|u - \Pi_h u\|_h \leq Ch(\|f\|_{L_2(\Omega)} + \|\varphi\|_{H^2(\Omega)})$$

$$(3.17) \quad \|u - \Pi_h u\|_{L_2(\Omega)} \leq Ch^2(\|f\|_{L_2(\Omega)} + \|\varphi\|_{H^2(\Omega)})$$

if  $\Omega$  is convex, and

$$(3.18) \quad \|u - \Pi_h u\|_h \leq C_\alpha h^\alpha (\|f\|_{L_2(\Omega)} + \|\varphi\|_{H^2(\Omega)})$$

$$(3.19) \quad \|u - \Pi_h u\|_{L_2(\Omega)} \leq C_\alpha h^{1+\alpha} (\|f\|_{L_2(\Omega)} + \|\varphi\|_{H^2(\Omega)})$$

if  $\Omega$  is nonconvex, where  $\alpha$  is the index of elliptic regularity that appears in (2.4).

We can then derive the following theorem using (3.14), (3.16) and (3.18).

THEOREM 3.4. For a quasi-uniform  $\mathcal{T}_h$  with mesh parameter  $h = \max_{T \in \mathcal{T}_h} h_T$ , we have

$$(3.20) \quad \|u - u_h\|_h \leq Ch(\|f\|_{L_2(\Omega)} + \|\varphi\|_{H^2(\Omega)})$$

if  $\Omega$  is convex, and

$$(3.21) \quad \|u - u_h\|_h \leq C_\alpha h^\alpha (\|f\|_{L_2(\Omega)} + \|\varphi\|_{H^2(\Omega)})$$

if  $\Omega$  is nonconvex and  $\alpha$  is the index of elliptic regularity that appears in (2.4).

For a nonconvex domain with corners  $c_1, \dots, c_L$ , a better error estimate can be obtained by using meshes that are graded around the reentrant corners of  $\Omega$ , i.e., meshes whose triangles satisfy the condition

$$(3.22) \quad h_T \approx \Phi_\mu(T)h \quad \forall T \in \mathcal{T}_h,$$

where the constants in the equivalence (3.22) are independent of  $h$ ,  $\mu = (\mu_1, \dots, \mu_L)$  is the vector containing the grading parameters, and the weight  $\Phi_\mu(T)$  is given by

$$(3.23) \quad \Phi_\mu(T) = \prod_{\ell=1}^L |c_\ell - c_T|^{1-\mu_\ell}.$$

Here  $c_T$  is the center of  $T$  and the grading parameters  $\mu_1, \dots, \mu_\ell$  are chosen according to

$$(3.24) \quad \begin{cases} \mu_\ell = 1 & \text{if } \omega_\ell < \pi \\ \mu_\ell < \pi/\omega_\ell & \text{if } \omega_\ell > \pi \end{cases}.$$

The choice (3.24) guarantees that

$$(3.25) \quad \int_0^1 r^{2(1-\mu_\ell)} (r^{(\pi/\omega_\ell)-2})^2 r \, dr < \infty.$$

It follows from (3.22) and (3.23) that

$$(3.26) \quad h_T \approx h^{1/\mu_\ell}$$

if the corner  $c_\ell$  is a vertex of  $T \in \mathcal{T}_h$ , and hence

$$(3.27) \quad |\ln h_T| \approx |\ln h| \quad \forall T \in \mathcal{T}_h,$$

where the constants in the equivalence (3.27) are independent of  $h$ . The construction of graded meshes that satisfy these conditions can be found for example in [23, 2, 1, 10, 5]. Note that, for any given grading parameters, the graded meshes satisfy the minimum angle condition and

$$(3.28) \quad \text{the number of triangles in a graded mesh } \mathcal{T}_h \text{ is proportional to } h^{-2}.$$

Below are the key estimates related to graded meshes.

Let  $\mathcal{T}_{h,\ell}$  be the collection of triangles in  $\mathcal{T}_h$  that touch a corner  $c_\ell$  of  $\Omega$ ,

$$\mathcal{T}'_h = \bigcup_{\omega_\ell > \pi} \mathcal{T}_{h,\ell} \quad \text{and} \quad \mathcal{T}''_h = \mathcal{T}_h \setminus \mathcal{T}'_h.$$

Then (2.1), (2.2), (2.5), (2.6) and (3.25) imply

$$(3.29) \quad \sum_{T \in \mathcal{T}''_h} [\Phi_\mu(T)]^2 |u|_{H^2(T)}^2 \leq C(\|f\|_{L_2(\Omega)}^2 + \|\varphi\|_{H^2(\Omega)}^2),$$

$$(3.30) \quad \sum_{T \in \mathcal{T}_{h,\ell}} |u|_{H^{1+\mu_\ell}(T)}^2 \leq C(\|f\|_{L_2(\Omega)}^2 + \|\varphi\|_{H^2(\Omega)}^2).$$

LEMMA 3.5. *Let  $\mathcal{T}_h$  be a graded mesh satisfying (3.22)–(3.24). The following interpolation error estimates are valid:*

$$(3.31) \quad \|u - \Pi_h u\|_h \leq Ch(\|f\|_{L_2(\Omega)} + \|\varphi\|_{H^2(\Omega)}),$$

$$(3.32) \quad \|u - \Pi_h u\|_{L_2(\Omega)} \leq Ch^2(\|f\|_{L_2(\Omega)} + \|\varphi\|_{H^2(\Omega)}).$$

*Proof.* On the one hand, we have by (3.10), (3.22) and (3.29),

$$(3.33) \quad \begin{aligned} \sum_{T \in \mathcal{T}''_h} \|\nabla(u - \Pi_h u)\|_{L_2(T)}^2 &\leq C \sum_{T \in \mathcal{T}''_h} h_T^2 |u|_{H^2(T)}^2 \\ &\leq Ch^2 \sum_{T \in \mathcal{T}''_h} [\Phi_\mu(T)]^2 |u|_{H^2(T)}^2 \leq Ch^2(\|f\|_{L_2(\Omega)}^2 + \|\varphi\|_{H^2(\Omega)}^2). \end{aligned}$$

On the other hand, we have by (3.10), (3.26) and (3.30),

$$(3.34) \quad \begin{aligned} \sum_{T \in \mathcal{T}'_h} \|\nabla(u - \Pi_h u)\|_{L_2(T)}^2 &\leq C \sum_{\omega_\ell > \pi} \sum_{T \in \mathcal{T}_{h,\ell}} h_T^{2\mu_\ell} |u|_{H^{1+\mu_\ell}(T)}^2 \\ &\leq Ch^2 \sum_{\omega_\ell > \pi} \sum_{T \in \mathcal{T}_{h,\ell}} |u|_{H^{1+\mu_\ell}(T)}^2 \leq Ch^2(\|f\|_{L_2(\Omega)}^2 + \|\varphi\|_{H^2(\Omega)}^2). \end{aligned}$$

Furthermore, it follows from (2.11) and (3.33)–(3.34) that

$$(3.35) \quad \begin{aligned} &\sum_{e \in \mathcal{E}_h} |e| \|\{\{\nabla(u - \Pi_h u)\}\}\|_{L_2(e)}^2 \\ &\leq Ch^2 \sum_{T \in \mathcal{T}''_h} [\Phi_\mu(T)]^2 |u|_{H^2(T)}^2 + Ch^2 \sum_{\omega_\ell > \pi} \sum_{T \in \mathcal{T}_{h,\ell}} |u|_{H^{1+\mu_\ell}(T)}^2 \\ &\leq Ch^2(\|f\|_{L_2(\Omega)}^2 + \|\varphi\|_{H^2(\Omega)}^2). \end{aligned}$$

The estimates (3.33)–(3.35) together with (3.15) imply (3.31).

Similarly, we have

$$\begin{aligned} \sum_{T \in \mathcal{T}_h''} \|u - \Pi_h u\|_{L_2(T)}^2 &\leq C \sum_{T \in \mathcal{T}_h''} h_T^4 |u|_{H^2(T)}^2 \\ &\leq Ch^4 \sum_{T \in \mathcal{T}_h''} [\Phi_\mu(T)]^2 |u|_{H^2(T)}^2 \leq Ch^4 (\|f\|_{L_2(\Omega)}^2 + \|\varphi\|_{H^2(\Omega)}^2), \end{aligned}$$

and

$$\begin{aligned} \sum_{T \in \mathcal{T}_h'} \|u - \Pi_h u\|_{L_2(T)}^2 &\leq C \sum_{\omega_\ell > \pi} \sum_{T \in \mathcal{T}_{h,\ell}} h_T^{2+2\mu_\ell} |u|_{H^{1+\mu_\ell}(T)}^2 \\ &\leq Ch^4 \sum_{\omega_\ell > \pi} \sum_{T \in \mathcal{T}_{h,\ell}} |u|_{H^{1+\mu_\ell}(T)}^2 \leq Ch^4 (\|f\|_{L_2(\Omega)}^2 + \|\varphi\|_{H^2(\Omega)}^2), \end{aligned}$$

which together imply (3.32).  $\square$

In view of (3.14) and (3.31), we have established the following theorem.

**THEOREM 3.6.** *Let  $\mathcal{T}_h$  be a graded mesh satisfying (3.22)–(3.24). The following discretization error estimate holds:*

$$\|u - u_h\|_h \leq Ch (\|f\|_{L_2(\Omega)} + \|\varphi\|_{H^2(\Omega)}).$$

**4.  $L_2$  Error estimates.** We can obtain a better estimate for the discretization error in the  $L_2$  norm through a duality argument.

**THEOREM 4.1.** *For a quasi-uniform mesh  $\mathcal{T}_h$ , we have*

$$(4.1) \quad \|u - u_h\|_{L_2(\Omega)} \leq Ch^2 (\|f\|_{L_2(\Omega)} + \|\varphi\|_{H^2(\Omega)})$$

if  $\Omega$  is convex, and

$$(4.2) \quad \|u - u_h\|_{L_2(\Omega)} \leq C_\alpha h^{2\alpha} (\|f\|_{L_2(\Omega)} + \|\varphi\|_{H^2(\Omega)})$$

if  $\Omega$  is nonconvex, where  $\alpha$  is the index of elliptic regularity that appears in (2.4).

If  $\Omega$  is nonconvex and  $\mathcal{T}_h$  is a graded mesh satisfying (3.22)–(3.24), we have

$$(4.3) \quad \|u - u_h\|_{L_2(\Omega)} \leq Ch^2 (\|f\|_{L_2(\Omega)} + \|\varphi\|_{H^2(\Omega)}).$$

*Proof.* Let  $\zeta \in H_0^1(\Omega)$  and  $\zeta_h \in V_h$  satisfy

$$(4.4) \quad a(v, \zeta) = \int_{\Omega} v(\Pi_h u - u_h) dx \quad \forall v \in H_0^1(\Omega),$$

$$(4.5) \quad a_h(v, \zeta_h) = \int_{\Omega} v(\Pi_h u - u_h) dx \quad \forall v \in V_h.$$

For a quasi-uniform mesh  $\mathcal{T}_h$ , it follows from (4.4)–(4.5), the symmetry of  $a(\cdot, \cdot)$  and  $a_h(\cdot, \cdot)$ , Lemma 3.3 and Theorem 3.4 that

$$(4.6) \quad \|\zeta - \Pi_h \zeta\|_h \leq Ch \|\Pi_h u - u_h\|_{L_2(\Omega)},$$

$$(4.7) \quad \|\zeta - \zeta_h\|_h \leq Ch \|\Pi_h u - u_h\|_{L_2(\Omega)},$$

if  $\Omega$  is convex, and

$$(4.8) \quad \|\zeta - \Pi_h \zeta\|_h \leq C_\alpha h^\alpha \|\Pi_h u - u_h\|_{L_2(\Omega)},$$

$$(4.9) \quad \|\zeta - \zeta_h\|_h \leq C_\alpha h^\alpha \|\Pi_h u - u_h\|_{L_2(\Omega)},$$

if  $\Omega$  is nonconvex.

For a graded mesh on a nonconvex domain, it follows from Theorem 3.6 that

$$(4.10) \quad \|\zeta - \Pi_h \zeta\|_h \leq Ch \|\Pi_h u - u_h\|_{L_2(\Omega)},$$

$$(4.11) \quad \|\zeta - \zeta_h\|_h \leq Ch \|\Pi_h u - u_h\|_{L_2(\Omega)}.$$

From (1.5), (3.3), (3.13) and (4.5) we see that

$$(4.12) \quad \begin{aligned} & \|\Pi_h u - u_h\|_{L_2(\Omega)}^2 = a_h(\Pi_h u - u_h, \zeta_h) \\ & = a_h(\Pi_h u - u_h, \zeta_h - \Pi_h \zeta) + a_h(\Pi_h u - u_h, \Pi_h \zeta) \\ & \leq \|\Pi_h u - u_h\|_h \|\zeta_h - \Pi_h \zeta\|_h - \int_\Omega f(\Pi_h \zeta) dx + a_h(\Pi_h u, \Pi_h \zeta). \end{aligned}$$

Furthermore, (1.1a), (1.6), Lemma 2.1 and (3.4) imply that

$$(4.13) \quad \begin{aligned} & - \int_\Omega f(\Pi_h \zeta) dx + a_h(\Pi_h u, \Pi_h \zeta) \\ & = - \int_\Omega f(\Pi_h \zeta) dx + a_h(\Pi_h u - u, \Pi_h \zeta) + a_h(u, \Pi_h \zeta) \\ & = \sum_{e \in \mathcal{E}_h} \int_e \{\{\nabla u\}\} \cdot \llbracket \Pi_h \zeta \rrbracket ds + a_h(\Pi_h u - u, \Pi_h \zeta). \end{aligned}$$

We can use (3.4) and (3.13) to estimate the first term on the right-hand side of (4.13) as follows:

$$(4.14) \quad \begin{aligned} & \sum_{e \in \mathcal{E}_h} \int_e \{\{\nabla u\}\} \cdot \llbracket \Pi_h \zeta \rrbracket ds = \sum_{e \in \mathcal{E}_h} \int_e \{\{\nabla(u - \Pi_h u)\}\} \cdot \llbracket \Pi_h \zeta \rrbracket ds \\ & = \sum_{e \in \mathcal{E}_h} \int_e \{\{\nabla(u - \Pi_h u)\}\} \cdot \llbracket \Pi_h \zeta - \zeta \rrbracket ds \\ & \leq \left( \sum_{e \in \mathcal{E}_h} |e| \|\{\{\nabla(u - \Pi_h u)\}\}\|_{L_2(e)}^2 \right)^{1/2} \left( \sum_{e \in \mathcal{E}_h} |e|^{-1} \|\llbracket \Pi_h \zeta - \zeta \rrbracket\|_{L_2(e)}^2 \right)^{1/2} \\ & \leq \|u - \Pi_h u\|_h \|\Pi_h \zeta - \zeta\|_h. \end{aligned}$$

For the second term on the right-hand side of (4.13), we have, by (3.12), (4.4) and Lemma 2.1 (applied to  $\zeta$ ),

$$(4.15) \quad \begin{aligned} a_h(\Pi_h u - u, \Pi_h \zeta) & = a_h(\Pi_h u - u, \Pi_h \zeta - \zeta) + a_h(\Pi_h u - u, \zeta) \\ & \leq \|\Pi_h u - u\|_h \|\Pi_h \zeta - \zeta\|_h + \int_\Omega (\Pi_h u - u)(\Pi_h u - u_h) dx \\ & \quad + \sum_{e \in \mathcal{E}_h} \int_e \llbracket \Pi_h u - u \rrbracket \{\{\nabla \zeta\}\} ds, \\ & \leq \|\Pi_h u - u\|_h \|\Pi_h \zeta - \zeta\|_h + \|\Pi_h u - u\|_{L_2(\Omega)} \|\Pi_h u - u_h\|_{L_2(\Omega)} \\ & \quad + \sum_{e \in \mathcal{E}_h} \int_e \llbracket \Pi_h u - u \rrbracket \{\{\nabla \zeta\}\} ds. \end{aligned}$$

It follows from (3.12) that, as in (4.14),

$$(4.16) \quad \sum_{e \in \mathcal{E}_h} \int_e [[\Pi_h u - u]] \{\{\nabla \zeta\}\} ds = \sum_{e \in \mathcal{E}_h} \int_e [[\Pi_h u - u]] \{\{\nabla(\zeta - \Pi_h \zeta)\}\} ds \\ \leq \|\zeta - \Pi_h \zeta\|_h \|\Pi_h u - u\|_h.$$

Combining (3.17), (3.19), Theorem 3.4, Lemma 3.5, Theorem 3.6 and (4.6)–(4.16), we find

$$(4.17) \quad \|\Pi_h u - u_h\|_{L_2(\Omega)} \leq Ch^2 (\|f\|_{L_2(\Omega)} + \|\varphi\|_{H^2(\Omega)})$$

if  $\Omega$  is convex and  $\mathcal{T}_h$  is quasi-uniform, or if  $\Omega$  is nonconvex and  $\mathcal{T}_h$  is a graded mesh satisfying (3.22)–(3.24), and

$$(4.18) \quad \|\Pi_h u - u_h\|_{L_2(\Omega)} \leq C_\alpha h^{2\alpha} (\|f\|_{L_2(\Omega)} + \|\varphi\|_{H^2(\Omega)})$$

if  $\Omega$  is nonconvex and  $\mathcal{T}_h$  is quasi-uniform.

The estimates (4.1)–(4.3) follow from (3.17), (3.19), (3.32) and (4.17)–(4.18).  $\square$

**5. A simple preconditioner.** Let  $A_h : V_h \rightarrow V'_h$  be the linear operator representing the bilinear form  $a_h(\cdot, \cdot)$ , i.e.,

$$(5.1) \quad \langle A_h w, v \rangle = a_h(w, v) \quad \forall v, w \in V_h,$$

where  $\langle \cdot, \cdot \rangle$  is the canonical bilinear form on  $V'_h \times V_h$ . In this section we construct a simple block diagonal preconditioner  $B_h$  for  $A_h$ .

Let the symmetric positive-definite bilinear form  $b_h(\cdot, \cdot)$  be defined by

$$(5.2) \quad b_h(w, v) = \sum_{T \in \mathcal{T}_h} \sum_{e \in \mathcal{E}_T} w_T(m_e) v_T(m_e) + \eta \sum_{e \in \mathcal{E}_h} \frac{1}{|e|^3} \int_e \Pi_e^0[[w]] \cdot \Pi_e^0[[v]] ds$$

for all  $v, w \in V_h$ , where  $\mathcal{E}_T$  is the set of the three edges of  $T$  and  $m_e$  is the midpoint of  $e$ , and let  $B_h : V_h \rightarrow V'_h$  be defined by

$$(5.3) \quad \langle B_h w, v \rangle = b_h(w, v) \quad \forall v, w \in V_h.$$

Note that the operator  $B_h$  is block diagonal with respect to the nodal basis associated with the midpoints of the edges of  $\mathcal{T}_h$  and its dual basis. This is due to the midpoint rule

$$\Pi_e^0 v = \frac{1}{|e|} \int_e v ds = v(m_e) \quad \forall v \in P_1(e),$$

which implies

$$\frac{1}{|e|^3} \int_e \Pi_e^0[[w]] \cdot \Pi_e^0[[v]] ds = \frac{w(e)v(e)}{|e|^2}$$

if  $e$  is a boundary edge and

$$\frac{1}{|e|^3} \int_e \Pi_e^0[[w]] \cdot \Pi_e^0[[v]] ds = \frac{1}{|e|^2} \left( w_1(m_e)v_1(m_e) + w_2(m_e)v_2(m_e) \right. \\ \left. - w_1(m_e)v_2(m_e) - w_2(m_e)v_1(m_e) \right)$$

if  $e$  is an interior edge shared by the triangles  $T_{e,1}$  and  $T_{e,2}$  and  $w_i = w|_{T_{e,i}}$  (resp.  $v_i = v|_{T_{e,i}}$ ) for  $i = 1, 2$ . In fact, the diagonal blocks are either  $1 \times 1$  (corresponding to the midpoints on  $\partial\Omega$ ) or  $2 \times 2$  (corresponding to the interior midpoints).

We begin by analyzing the operator  $B_h^{-1}A_h$  for quasi-uniform meshes.

LEMMA 5.1. *For a quasi-uniform mesh  $\mathcal{T}_h$ , we have*

$$(5.4) \quad \frac{\lambda_{\max}(B_h^{-1}A_h)}{\lambda_{\min}(B_h^{-1}A_h)} \leq Ch^{-2}.$$

*Proof.* From the obvious estimate

$$\|\nabla v\|_{L_2(T)}^2 \leq C \sum_{e \in \mathcal{E}_T} v^2(m_e)$$

we have

$$\langle A_h v, v \rangle \leq C \langle B_h v, v \rangle \quad \forall v \in V_h,$$

and hence, by the Rayleigh quotient formula [22],

$$(5.5) \quad \lambda_{\max}(B_h^{-1}A_h) = \max_{v \in V_h \setminus \{0\}} \frac{\langle A_h v, v \rangle}{\langle B_h v, v \rangle} \leq C.$$

In the other direction, we first observe that the quasi-uniformity of  $\mathcal{T}_h$  implies

$$(5.6) \quad h_T \approx h \approx |e| \quad \forall T \in \mathcal{T}_h \quad \text{and} \quad \forall e \in \mathcal{E}_h.$$

It then follows from the Poincaré-Friedrichs inequality for piecewise  $H^1$  functions [8] that

$$(5.7) \quad \|v\|_{L_2(\Omega)}^2 \leq C \left( \sum_{T \in \mathcal{T}_h} \|\nabla v\|_{L_2(T)}^2 + \sum_{e \in \mathcal{E}_h} |e|^{-1} \|\Pi_e^0[v]\|_{L_2(e)}^2 \right) \quad \forall v \in V_h,$$

which together with (1.4), (3.2), (5.1)–(5.3) and (5.6) imply that

$$h^2 \langle B_h v, v \rangle \leq C \langle A_h v, v \rangle \quad \forall v \in V_h.$$

Hence, by the Rayleigh quotient formula, we have

$$(5.8) \quad \lambda_{\min}(B_h^{-1}A_h) = \min_{v \in V_h \setminus \{0\}} \frac{\langle A_h v, v \rangle}{\langle B_h v, v \rangle} \geq Ch^2.$$

The estimate (5.4) follows from (5.5) and (5.8).  $\square$

Next we analyze the operator  $B_h^{-1}A_h$  for graded meshes.

LEMMA 5.2. *For a graded mesh  $\mathcal{T}_h$ , we have*

$$(5.9) \quad \frac{\lambda_{\max}(B_h^{-1}A_h)}{\lambda_{\min}(B_h^{-1}A_h)} \leq Ch^{-2}(1 + |\ln h|).$$

*Proof.* Since the estimate (5.5) remains valid, we only need an estimate for  $\lambda_{\min}(B_h^{-1}A_h)$ . Observe that, because of (3.28),

$$(5.10) \quad \sum_{T \in \mathcal{T}_h} \sum_{e \in \mathcal{E}_T} v^2(m_e) \leq 3 \|v\|_{L_\infty(\Omega)}^2 \sum_{T \in \mathcal{T}_h} 1 \leq Ch^{-2} \|v\|_{L_\infty(\Omega)}^2 \quad \forall v \in V_h.$$

Furthermore we have the following discrete Sobolev inequality [9]

$$(5.11) \quad \|v\|_{L^\infty(\Omega)}^2 \leq C(1 + |\ln h|) \left( \sum_{T \in \mathcal{T}_h} \|v\|_{H^1(T)}^2 + \sum_{e \in \mathcal{E}_h} |e|^{-1} \|\Pi_e^0[v]\|_{L_2(e)}^2 \right)$$

for all  $v \in V_h$ . (The result in [9] was derived under the assumption that  $\mathcal{T}_h$  is quasi-uniform. But the proof also applies to the case where  $\mathcal{T}_h$  is regular and (3.27) holds.)

Combining (1.4), (3.2), (5.1)–(5.3), (5.7), and (5.10)–(5.11), we find

$$\langle B_h v, v \rangle \leq Ch^{-2}(1 + |\ln h|) \langle A_h v, v \rangle \quad \forall v \in V_h,$$

which implies through the Rayleigh quotient formula

$$(5.12) \quad \lambda_{\min}(B_h^{-1}A_h) \geq Ch^2(1 + |\ln h|)^{-1}.$$

The estimate (5.9) follows from (5.5) and (5.12).  $\square$

REMARK 5.3. The condition number estimate (5.9) is identical with the condition number estimate for conforming finite element methods on graded meshes [6].

**6. Extensions.** The results in previous sections can be extended to a grid  $\mathcal{T}_h$  with hanging nodes. We assume that if an edge of a triangle in  $\mathcal{T}_h$  contains a hanging node, then it is subdivided by the edges of other triangles in  $\mathcal{T}_h$ . An example of such a grid is depicted in Figure 6.1.

For such grids the only modification of (1.6) occurs in the definition of  $\mathcal{E}_h$ . An (open) edge of a triangle in  $\mathcal{T}_h$  belongs to  $\mathcal{E}_h$  if and only if it satisfies one of the following conditions: (i) it contains a hanging node, (ii) it is a subset of  $\partial\Omega$ , or (iii) it is the common edge of two triangles in  $\mathcal{T}_h$ . Then the interpolation operator  $\Pi_h$  defined by (3.11) still satisfies (3.12)–(3.13) and the analysis in Section 3 and Section 4 remains valid.

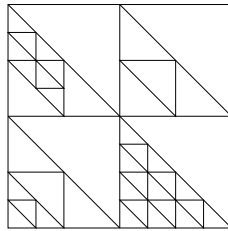


FIG. 6.1. Example of a grid with hanging nodes

Under the new definition of  $\mathcal{E}_h$ , the preconditioner  $B_h$  defined by (5.2) and (5.3) is still a block diagonal preconditioner and the condition number estimates in Section 5 remain valid. (The constants in the estimates will depend on the maximum number of hanging nodes that can appear on any edge.) But now the block corresponding to an edge  $e$  with hanging nodes is  $n \times n$ , where  $n$  is the number of midpoints (of edges of triangles of  $\mathcal{T}_h$ ) that belong to  $e$ . For example, for the edge in Figure 6.1 that connects the center to the lower right corner, the corresponding diagonal block is  $5 \times 5$  (one midpoint from the large triangle and four midpoints from the small triangles).

The WOPSIP method can also be applied to elliptic boundary value problems with variable coefficients that are Lipschitz continuous. Consider the problem where the bilinear form  $a(\cdot, \cdot)$  in (1.1a) is defined by

$$a(w, v) = \int_{\Omega} [(\mathbf{K}\nabla w) \cdot \nabla v + bwv] dx.$$

Here  $\mathbf{K}(x)$  is a Lipschitz continuous  $2 \times 2$ -matrix-valued function on  $\bar{\Omega}$  such that

$$\mathbf{K}(x)\mathbf{z} \cdot \mathbf{z} \geq c\mathbf{z} \cdot \mathbf{z} \quad \forall x \in \bar{\Omega}, \mathbf{z} \in \mathbb{R}^2,$$

where  $c > 0$  is a constant independent of  $x$  and  $\mathbf{z}$ , and  $b(x)$  is a Lipschitz continuous nonnegative scalar function defined on  $\bar{\Omega}$ . The corresponding bilinear form for the WOPSIP method is then given by

$$a_h(w, v) = \sum_{T \in \mathcal{T}_h} \int_T [(\mathbf{K}\nabla w) \cdot \nabla v + bwv] dx + \eta \sum_{e \in \mathcal{E}_h} \frac{1}{|e|^3} \int_e \Pi_e^0[[w]] \cdot \Pi_e^0[[v]] ds.$$

The results in Section 3 and Section 4 also hold for this problem. The only significant modification occurs in the handling of the analog of (3.7):

$$\begin{aligned} (6.1) \quad a_h(u - u_h, w) &= \sum_{e \in \mathcal{E}_h} \int_e \mathbf{K}\nabla u \cdot [[w]] ds \\ &= \sum_{e \in \mathcal{E}_h} \int_e \bar{\mathbf{K}}\nabla u \cdot [[w]] ds + \sum_{e \in \mathcal{E}_h} \int_e (\mathbf{K} - \bar{\mathbf{K}})\nabla u \cdot [[w]] ds \end{aligned}$$

where, on each  $e \in \mathcal{E}_h$ ,  $\bar{\mathbf{K}}$  denotes the mean value of  $\mathbf{K}$  on  $e$ .

We can proceed as in Section 3 to obtain the following estimate for the first term on the right-hand side of (6.1):

$$(6.2) \quad \sum_{e \in \mathcal{E}_h} \int_e \bar{\mathbf{K}}\nabla u \cdot [[w]] ds \leq C \left[ \|u - v\|_h + h(\|f\|_{L_2(\Omega)} + \|\varphi\|_{H^2(\Omega)}) \right] \|w\|_h \quad \forall v \in V_h.$$

The second term on the right-hand side of (6.1) can be estimated as follows:

$$\begin{aligned} &\sum_{e \in \mathcal{E}_h} \int_e (\mathbf{K} - \bar{\mathbf{K}})\nabla u \cdot [[w]] ds \\ &\leq C \sum_{e \in \mathcal{E}_h} |e| \|\nabla u\|_{L_2(e)} \|[[w]]\|_{L_2(e)} \\ (6.3) \quad &\leq Ch \left( \sum_{e \in \mathcal{E}_h} |e| \|\nabla u\|_{L_2(e)}^2 \right)^{1/2} \left( \sum_{e \in \mathcal{E}_h} |e|^{-1} \|[[w]]\|_{L_2(e)}^2 \right)^{1/2} \\ &\leq Ch(\|f\|_{L_2(\Omega)} + \|\varphi\|_{H^2(\Omega)}) \|w\|_h, \end{aligned}$$

where we have used (2.12), (3.1), and Lemma 3.1.

It follows from the estimates (6.2)–(6.3) that Lemma 3.2 remains valid. The modifications for the proofs of Theorem 3.4, Theorem 3.6 and Theorem 4.1 are straightforward. Note that for a nonconvex domain the singularity of the solution  $u$  at a reentrant corner depends on the value of  $\mathbf{K}$  at that corner. But we can still obtain optimal error estimates in both the  $\|\cdot\|_h$  norm and the  $L_2$  norm by choosing the grading factor  $\mu_\ell$  at any reentrant corner to be less than  $1/2$ .

REMARK 6.1. The WOPSIP method can also be applied to mixed (Dirichlet and Neumann) boundary conditions. The analysis is similar but more complicated, since singularities also appear in the neighborhood of points on  $\partial\Omega$  where the boundary condition changes type.

**7. Numerical results.** In this section we report the results of some numerical experiments involving the WOPSIP method. The computation is performed using the nodal bases associated with the midpoints of the edges of the triangles.

In the first set of experiments we take  $\Omega$  to be the unit square  $(0, 1) \times (0, 1)$  and the exact solution of (1.1) to be

$$u(x, y) = xy(1 - x)(1 - y).$$

We solve (1.1) using the WOPSIP method with different penalty parameters  $\eta = 0.1, 1, 10$  and 100, on uniform grids  $\mathcal{T}_1, \dots, \mathcal{T}_8$ , where the length of a horizontal/vertical edge in  $T_k$  is  $h_k = 2^{-k}$ . The relative errors

$$\varepsilon_k = \frac{\sqrt{\sum_{T \in \mathcal{T}_k} \|\nabla(u - u_k)\|_{L_2(T)}^2}}{\|\nabla u\|_{L_2(\Omega)}}$$

in the piecewise  $H^1$  semi-norm and the relative errors

$$\lambda_k = \frac{\|u - u_k\|_{L_2(\Omega)}}{\|u\|_{L_2(\Omega)}}$$

in the  $L_2$  norm are computed. The results are presented in Table 7.1. The error bounds (3.20) and (4.1) are clearly visible. Furthermore, the constant in the  $H^1$  error bound is relatively independent of  $\eta$  when  $h_k$  is small. On the other hand, the constant in the  $L_2$  error bound becomes noticeably smaller as  $\eta$  increases.

TABLE 7.1  
*Relative errors on  $\Omega$  in the piecewise  $H^1$  semi-norm and the  $L_2$  norm for  $1 \leq k \leq 8$  and  $\eta = 0.1, 1, 10$  and 100.*

$k$	$\eta = 0.1$		$\eta = 1$		$\eta = 10$		$\eta = 100$	
	$\varepsilon_k/h_k$	$\lambda_k/h_k^2$	$\varepsilon_k/h_k$	$\lambda_k/h_k^2$	$\varepsilon_k/h_k$	$\lambda_k/h_k^2$	$\varepsilon_k/h_k$	$\lambda_k/h_k^2$
1	1.092	33.863	0.659	4.030	0.403	0.700	0.392	0.401
2	1.687	29.665	0.545	3.827	0.373	0.767	0.370	0.514
3	1.644	30.129	0.434	3.628	0.372	0.785	0.371	0.572
4	1.113	30.895	0.390	3.495	0.373	0.784	0.372	0.588
5	0.680	30.941	0.377	3.420	0.373	0.779	0.373	0.592
6	0.473	30.778	0.374	3.381	0.373	0.776	0.373	0.593
7	0.400	30.640	0.373	3.361	0.373	0.775	0.373	0.593
8	0.380	30.556	0.373	3.350	0.373	0.739	0.373	0.566

We also compute the condition number  $\kappa(B_k^{-1}A_k)$  for  $1 \leq k \leq 8$  and  $\eta = 0.1, 1, 10$  and 100. The numbers  $h_k^2 \kappa(B_k^{-1}A_k)$ , tabulated in Table 7.2, clearly demonstrate the estimate (5.4).

In the second set of experiments we analyze the performance of the WOPSIP method on some nonconforming partitions of the unit square. This is a first step in evaluating the effectiveness of an adaptive mesh refinement algorithm.

We consider three different nonconforming partitions of the unit square. The first three levels of mesh refinement for each of these partitions is shown in Figure 7.1–Figure 7.3. The methodology for the first two nonconforming partitions is simple. The coarsest mesh ( $k = 0$ ) is given and each subsequent mesh is obtained by uniform subdivision. The mesh refinement in the third nonconforming partition is slightly more complicated. The  $k^{\text{th}}$  level

TABLE 7.2  
 $h_k^2 \kappa(B_k^{-1} A_k)$  for  $1 \leq k \leq 8$  and  $\eta = 0.1, 1, 10$  and  $100$ .

$k$	$\eta = 0.1$	$\eta = 1$	$\eta = 10$	$\eta = 100$
1	17.6	3.87	2.10	1.77
2	5.18	2.23	1.84	1.80
3	2.67	1.91	1.83	1.82
4	2.04	1.84	1.82	1.82
5	1.88	1.83	1.82	1.82
6	1.84	1.83	1.82	1.82
7	1.83	1.82	1.82	1.82
8	1.83	1.82	1.82	1.82

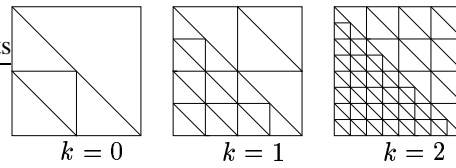


FIG. 7.1. First three levels of the first nonconforming partition on  $\Omega$ .

is obtained from the  $(k - 1)^{\text{st}}$  level by refining the largest triangles in the partition and the lower left triangle. In all cases refinement on any particular triangle is obtained by connecting the midpoints of the edges of that triangle. Also, the length of the longest horizontal/vertical edge is  $h_k = 2^{-k}$  for all of the partitions considered.

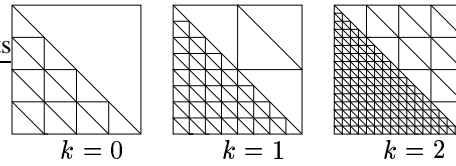


FIG. 7.2. First three levels of the second nonconforming partition on  $\Omega$ .

We have compared the relative errors of the conforming triangulation with those of the three nonconforming partitions. Since the dependence on  $\eta$  in each of the nonconforming partitions is very similar to the dependence in the conforming triangulation, we present the numerical results only for  $\eta = 1$  in Table 7.3 and Table 7.4.

In view of Figure 7.1, we expect the error for the first nonconforming partition at level  $k$  to be smaller than the conforming triangulation at level  $k$ , but larger than the conforming triangulation at level  $k + 1$ . The results in Table 7.3 and Table 7.4 demonstrate this result. Furthermore, Figure 7.2 suggests that the errors of the second nonconforming partition at level  $k$  should be between the errors of the conforming triangulation at levels  $k$  and  $k + 2$ . This is confirmed by the numerical results. Finally, from Figure 7.3 we expect that the errors for the third nonconforming partition at level  $k$  should be less than or equal to the errors of the conforming triangulation at that same level. The numerical results very nearly satisfy this observation.

In addition, we have computed the condition number  $\kappa(B_k^{-1} A_k)$  for the second nonconforming partition for  $0 \leq k \leq 7$  and  $\eta = 0.1, 1, 10$  and  $100$ . The numbers  $h_k^2 \kappa(B_k^{-1} A_k)$  are tabulated in Table 7.5. The estimate (5.4) is clearly demonstrated as it was with the conform-

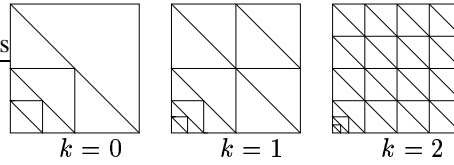


FIG. 7.3. First three levels of the third nonconforming partition on  $\Omega$ .

TABLE 7.3

*Comparison of relative errors in the piecewise  $H^1$  semi-norm of the nonconforming partitions and the conforming triangulation ( $\eta = 1$ ).*

$k$	NC1	NC2	NC3	C
0	5.49E-01	5.48E-01	2.51E+00	–
1	2.86E-01	2.90E-01	5.32E-01	3.30E-01
2	1.20E-01	1.24E-01	1.99E-01	1.36E-01
3	4.59E-02	4.56E-02	6.83E-02	5.42E-02
4	1.98E-02	1.88E-02	2.67E-02	2.44E-02
5	9.39E-03	8.74E-03	1.21E-02	1.18E-02
6	4.63E-03	4.29E-03	5.88E-03	5.84E-03
7	2.31E-03	2.13E-03	2.92E-03	2.91E-03
8	–	–	–	1.46E-03

ing triangulation, however, the constant is larger in the nonconforming case.

Our numerical results suggest that the WOPSIP method will work well when implemented using an adaptive mesh refinement algorithm. The introduction of hanging nodes has seemingly no adverse effects on the method’s performance, which is a very attractive feature of this method.

In our final set of numerical experiments we solve (1.1) on the L-shaped domain  $\Omega_L$  with vertices  $(-1, -1)$ ,  $(1, -1)$ ,  $(1, 0)$ ,  $(0, 0)$ ,  $(0, 1)$  and  $(-1, 1)$ . The exact (singular) solution is

$$(7.1) \quad u = r^{2/3} \sin\left(\frac{2}{3}\left(\theta - \frac{\pi}{2}\right)\right),$$

where  $(r, \theta)$  are the standard polar coordinates. As on the unit square we solve (1.1) using the WOPSIP method with varying penalty parameters  $\eta = 0.1, 1, 10$  and  $100$ , on uniform and graded meshes  $\mathcal{T}_0, \dots, \mathcal{T}_7$  (cf. Figure 7 where  $\mathcal{T}_2$  is depicted for both the uniform mesh and the graded mesh). The mesh parameter is  $h_k = 2^{-k}$ .

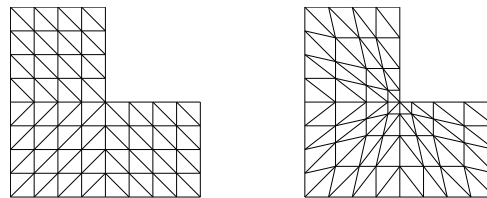


FIG. 7.4. Uniform and graded meshes on the L-shaped domain  $\Omega_L$

Let  $\mathcal{I}_k u \in V_k$  be the piecewise linear interpolant that agrees with  $u$  at all the midpoints

TABLE 7.4

*Comparison of relative errors in the  $L_2$  norm of the nonconforming partitions and the conforming triangulation ( $\eta = 1$ ).*

$k$	NC 1	NC2	NC3	C
0	2.81E+00	2.60E+00	2.41E+01	–
1	6.48E–01	5.80E–01	1.09E+00	1.01E+00
2	1.50E–01	1.31E–01	2.53E–01	2.39E–01
3	3.59E–02	3.13E–02	5.81E–02	5.67E–02
4	8.68E–03	7.57E–03	1.38E+02	1.37E–02
5	2.13E–03	1.85E–03	3.35E–03	3.34E–03
6	5.26E–04	4.58E–04	8.26E–04	8.25E–04
7	1.31E–04	1.14E–04	2.05E–04	2.05E–04
8	–	–	–	5.11E–05

TABLE 7.5

*$h_k^2 \kappa(B_k^{-1} A_k)$  for  $0 \leq k \leq 7$  and  $\eta = 0.1, 1, 10$  and  $100$  on the second nonconforming partition.*

$k$	$\eta = 0.1$	$\eta = 1$	$\eta = 10$	$\eta = 100$
0	84.22	34.31	25.41	22.68
1	41.23	26.37	22.14	21.41
2	28.25	21.48	20.15	19.99
3	22.59	20.04	19.71	19.68
4	20.42	19.69	19.61	19.60
5	19.79	19.60	19.58	19.58
6	19.63	19.58	19.58	19.57
7	19.58	19.57	19.57	19.57

of the edges of  $\mathcal{T}_k$ . For convenience we have computed the absolute errors

$$\varepsilon_k^s = \left( \sum_{T \in \mathcal{T}_k} \|\nabla(\mathcal{I}_k u - u_k)\|_{L_2(T)}^2 \right)^{1/2}$$

in the piecewise  $H^1$  semi-norm and the absolute errors

$$\lambda_k^s = \|\mathcal{I}_k u - u_k\|_{L_2(\Omega_L)}$$

in the  $L_2$  norm. The rate of convergence is given by  $\alpha_k^s = \log_2(\varepsilon_{k-1}^s / \varepsilon_k^s)$  for the piecewise  $H^1$  semi-norm and by  $\beta_k^s = \log_2(\lambda_{k-1}^s / \lambda_k^s)$  for the  $L_2$  norm.

The results for uniform meshes with  $\eta = 1$  are presented in Table 7.6. The asymptotic convergence rate of  $2/3$  (resp.  $4/3$ ) in the piecewise  $H^1$  semi-norm (resp. the  $L_2$  norm) predicted by Theorem 3.4 (resp. Theorem 4.1) is clearly demonstrated. The results for graded meshes with  $\eta = 1$  are presented in Table 7.7, and it is clear that the convergence rate is 1 in the piecewise  $H^1$  semi-norm and 2 in the  $L_2$  norm, as predicted by Theorem 3.6 and Theorem 4.1. The dependence on  $\eta$  is very similar to the dependence observed for the unit square, so we have omitted those results.

**8. Concluding remarks.** We have developed a weakly over-penalized symmetric interior penalty (WOPSIP) method that satisfies optimal order error estimates in both the energy norm and the  $L_2$  norm. This method is stable for any positive penalty parameter, as long as it is bounded away from zero. At the same time, there exists a simple block-diagonal preconditioner for the resulting discrete system so that it behaves like a typical discrete system for a second order elliptic boundary value problem.

TABLE 7.6

Absolute errors and convergence rates on  $\Omega_L$  with uniform meshes in the piecewise  $H^1$  semi-norm and the  $L_2$  norm for  $0 \leq k \leq 7$  and  $\eta = 1$ .

$k$	$\varepsilon_k^s$	$\alpha_k^s$	$\lambda_k^s$	$\beta_k^s$
0	1.04E+00	—	2.78E−01	—
1	6.42E−01	0.694	1.24E−01	1.166
2	2.63E−01	1.288	4.07E−02	1.605
3	9.73E−02	1.435	1.25E−02	1.701
4	4.70E−02	1.048	4.10E−03	1.610
5	2.79E−02	0.752	1.44E−03	1.513
6	1.74E−02	0.678	5.28E−04	1.446
7	1.10E−02	0.667	1.99E−04	1.403

TABLE 7.7

Absolute errors and convergence rates on  $\Omega_L$  with graded meshes in the piecewise  $H^1$  semi-norm and the  $L_2$  norm for  $0 \leq k \leq 7$  and  $\eta = 1$ .

$k$	$\varepsilon_k^s$	$\alpha_k^s$	$\lambda_k^s$	$\beta_k^s$
0	1.04E+00	—	2.78E−01	—
1	7.01E−01	0.567	1.12E−01	1.308
2	3.47E−01	1.017	4.22E−02	1.411
3	1.22E−01	1.503	1.26E−02	1.744
4	4.18E−02	1.548	3.41E−03	1.886
5	1.76E−02	1.249	8.98E−04	1.923
6	8.73E−03	1.012	2.35E−04	1.932
7	4.56E−03	0.938	6.15E−05	1.936

The results in this paper provide the foundation for the study of fast solvers for second order elliptic boundary value problems based on the WOPSIP formulation [17, 25], which will complement the work in [16, 15] that is based on a weakly over-penalized nonsymmetric interior penalty (WOPNIP) formulation.

It is well-known that the conforming  $P_1$  finite element method does not work for either the time-harmonic (frequency-domain) Maxwell equations or the Maxwell eigenproblem. But there are methods [13, 12, 11, 14] based on weakly continuous  $P_1$  vector fields that do work for such problems. Therefore the techniques developed in this paper and [16, 15, 17] are also relevant for problems in computational electromagnetics.

## REFERENCES

- [1] TH. APEL, *Anisotropic Finite Elements*, Teubner, Stuttgart, 1999.
- [2] TH. APEL, A.-M. SÄNDIG, AND J. R. WHITEMAN, *Graded mesh refinement and error estimates for finite element solutions of elliptic boundary value problems in non-smooth domains*, Math. Methods Appl. Sci., 19 (1996), pp. 63–85.
- [3] D. N. ARNOLD, *An interior penalty finite element method with discontinuous elements*, SIAM J. Numer. Anal., 19 (1982), pp. 742–760.
- [4] D. N. ARNOLD, F. BREZZI, B. COCKBURN, AND L. D. MARINI, *Unified analysis of discontinuous Galerkin methods for elliptic problems*, SIAM J. Numer. Anal., 39 (2001/2002) pp. 1749–1779.
- [5] C. BĂCUȚĂ, V. NISTOR, AND L. T. ZIKATANOV, *Improving the rate of convergence of ‘high order finite elements’ on polygons and domains with cusps*, Numer. Math., 100 (2005), pp.165–184.
- [6] R. E. BANK AND L. R. SCOTT, *On the conditioning of finite element equations with highly refined meshes*, SIAM J. Numer. Anal., 26 (1989), pp. 1383–1394.
- [7] F. BASSI, S. REBAY, G. MARIOTTI, S. PEDINOTTI, AND M. SAVINI, *A high-order accurate discontinuous*

- finite element method for inviscid and viscous turbomachinery flows*, in Proceedings of 2nd European Conference on Turbomachinery, Fluid Dynamics and Thermodynamics, R. Decuyper and G. Dibelius, eds., Technologisch Instituut, Antwerpen, Belgium, 1997, pp. 99–108.
- [8] S. C. BRENNER, *Poincaré-Friedrichs inequalities for piecewise  $H^1$  functions*, SIAM J. Numer. Anal., 41 (2003), pp. 306–324.
- [9] S. C. BRENNER, *Discrete Sobolev and Poincaré inequalities for piecewise polynomial functions*, Electron. Trans. Numer. Anal., 18 (2004), pp. 42–48.  
<http://etna.math.kent.edu/vol.18.2004/pp42-48.dir/pp42-48.html>.
- [10] S. C. BRENNER AND C. CARSTENSEN, *Finite Element Methods*, in Encyclopedia of Computational Mechanics, E. Stein, R. de Borst, and T. J. R. Hughes, eds., Wiley, Weinheim, 2004, pp. 73–118.
- [11] S. C. BRENNER, J. CUI, F. LI, AND L.-Y. SUNG, *A nonconforming finite element method for a two-dimensional curl-curl and grad-div problem*, preprint, 2007, to appear in: Numer. Math..
- [12] S. C. BRENNER, F. LI, AND L.-Y. SUNG, *A locally divergence-free interior penalty method for two dimensional curl-curl problems*, SIAM J. Numer. Anal., 46 (2008), pp. 1190–1211.
- [13] S. C. BRENNER, F. LI, AND L.-Y. SUNG, *A locally divergence-free nonconforming finite element method for the time-harmonic Maxwell equations*, Math. Comp., 76 (2007), pp. 573–595.
- [14] S. C. BRENNER, F. LI, AND L.-Y. SUNG, *A nonconforming penalty method for a two dimensional curl-curl problem*, preprint, 2007.
- [15] S. C. BRENNER AND L. OWENS, *A W-cycle algorithm for a weakly over-penalized interior penalty method*, Comput. Methods Appl. Mech. Engrg., 196 (2007), pp. 3823–3832.
- [16] S. C. BRENNER AND L. OWENS, *A weakly over-penalized nonsymmetric interior penalty method*, JNAIAM, 2 (2007), pp. 35–48.
- [17] S. C. BRENNER, L. OWENS, AND L.-Y. SUNG, *Multigrid methods for weakly over-penalized symmetric interior penalty methods*, in preparation.
- [18] S. C. BRENNER AND L. R. SCOTT, *The Mathematical Theory of Finite Element Methods*, Third ed., Springer, New York, 2008.
- [19] P. G. CIARLET, *The Finite Element Method for Elliptic Problems*, North-Holland, Amsterdam, 1978.
- [20] M. CROUZEIX AND P.-A. RAVIART, *Conforming and nonconforming finite element methods for solving the stationary Stokes equations I*, RAIRO Anal. Numér., 7 (1973), pp. 33–75.
- [21] M. DAUGE, *Elliptic Boundary Value Problems on Corner Domains*, Lecture Notes in Mathematics 1341, Springer, Berlin-Heidelberg, 1988.
- [22] G. H. GOLUB AND C. F. VAN LOAN, *Matrix Computations*, Third ed., The Johns Hopkins University Press, Baltimore, 1996.
- [23] P. GRISVARD, *Elliptic Problems in Non Smooth Domains*, Pitman, Boston, 1985.
- [24] S. A. NAZAROV AND B. A. PLAMENEVSKY, *Elliptic Problems in Domains with Piecewise Smooth Boundaries*, de Gruyter, Berlin-New York, 1994.
- [25] L. OWENS, *Multigrid Methods for Weakly Over-Penalized Interior Penalty Methods*, PhD thesis, Department of Mathematics, University of South Carolina, 2007.
- [26] B. RIVIÈRE, M. F. WHEELER, AND V. GIRAULT, *A priori error estimates for finite element methods based on discontinuous approximation spaces for elliptic problems*, SIAM J. Numer. Anal., 39 (2001), pp. 902–931.
- [27] M. F. WHEELER, *An elliptic collocation-finite-element method with interior penalties*, SIAM J. Numer. Anal., 15 (1978), pp. 152–161.